

Uppermost mantle anisotropy beneath the southern Laurentian margin: Evidence from Knippa peridotite xenoliths, Texas

Takako Satsukawa,¹ Katsuyoshi Michibayashi,^{1,2} Urmidola Raye,³ Elizabeth Y. Anthony,⁴ Jay Pulliam,⁵ and Robert Stern³

Received 2 July 2010; revised 7 September 2010; accepted 13 September 2010; published 27 October 2010.

[1] Peridotite xenoliths from southern Texas consist of spinel lherzolite, harzburgite and minor dunite. Based on phase relations and temperature of equilibration, Knippa xenoliths come from the uppermost mantle, 40–70 km deep. Knippa xenoliths provide rare snapshots of upper mantle processes and compositions beneath south-central Laurentia. They preserve olivine a-axis fiber fabrics with a strong concentration of [100] and girdles of [010] and [001]. Assuming a lithospheric mantle having a horizontal flow direction parallel to fast directions, the mantle lithospheric fabric revealed by the xenoliths mostly explains the magnitude of observed shear-wave splitting observed along the southern margin of the Laurentian craton. **Citation:** Satsukawa, T., K. Michibayashi, U. Raye, E. Y. Anthony, J. Pulliam, and R. Stern (2010), Uppermost mantle anisotropy beneath the southern Laurentian margin: Evidence from Knippa peridotite xenoliths, Texas, *Geophys. Res. Lett.*, 37, L20312, doi:10.1029/2010GL044538.

1. Introduction

[2] The nature of ocean-continent transitional lithosphere is complicated. Recent passive seismological investigations provide fruitful avenues of inexpensive research to begin interrogating the lithosphere. Measuring shear-wave splitting (SKS) images the orientation and degree of polarization of mantle fabrics, and constrain models for the formation of these fabrics, including the mantle beneath south central North America [Gao *et al.*, 2008]. In spite of the robustness of SKS measurements, it is often not clear if anisotropy inferred from these measurements resides in the mantle lithosphere or asthenosphere [Fouch and Rondenay, 2006]. Here we are interested in understanding fabrics for mantle xenoliths from southern Texas, and use this information to understand shear-wave splitting for upper mantle beneath the northern margin of the Gulf of Mexico (GoM) (Figure 1). A previous study documented significant shear wave splitting beneath this region, with fast directions parallel to the Texas GoM continental margin (Figure 1) [Gao *et al.*, 2008]. They noted that SKS splitting reached an apparent maximum where the crust was thinnest and discussed the parallelism of

the observed mantle anisotropy and the SE edge of the Laurentian cratonic keel.

[3] In this study, we present new SKS results and petro-fabric data for spinel peridotite xenoliths from Knippa, Texas, and use these results illuminate the origin and significance of shear wave splitting beneath southern Laurentia (Figure 1). The seismic anisotropy resulting mainly from olivine crystallographic preferred orientations (CPO) tends to show a maximum seismic velocity parallel to the direction of plastic flow within the upper mantle [Nicolas and Christensen, 1987]. Assuming that shear-wave splitting reflects mineral CPO, we can use CPO measured in mantle xenoliths to better understand uppermost mantle structure beneath south central North America and the elastic coefficients of minerals to evaluate the delay time along ray paths.

2. Geological Setting

[4] A quarry near Knippa, Texas (Figure 1) exposes Late Cretaceous basanites containing upper mantle xenoliths. This is the only known mantle peridotite locality in Texas [Young and Lee, 2009]. Mantle xenoliths were carried up by Late Cretaceous (~87 Ma) quite primitive nephelinites of the Balcones Igneous Province (BIP) [Griffin *et al.*, 2010]. BIP volcanoes approximate the boundary between the ~1.1–1.4 Ga southernmost Laurentian (Texas) craton and Jurassic age transitional lithosphere along the GoM margin. The transitional lithosphere also involves the deformed rocks of the Ouachita fold belt [Keller *et al.*, 1989].

[5] Knippa peridotites are spinel lherzolite and harzburgite (plus minor dunite) consisting of olivine (Ol), orthopyroxene (Opx), clinopyroxene (Cpx) and spinel (Sp). Minerals have high Mg#: Ol (F_{0.89–0.91.6}), Opx (En_{89.3–92.3}) and Cpx (Mg# = 90.4–93.4). Cr# (atomic Cr/(Cr+Al)) in Sp show moderate depletion, ranging from 0.14–0.21 for lherzolite to 0.25–0.36 for harzburgite, indicating that lherzolite experienced 5–9% melt depletion compared to 11–14% for harzburgite. Temperatures determined using the Ca in Opx thermometer [Brey and Kohler, 1990] range between 900 and 1000°C. Based on the ubiquitous presence of spinel and absence of garnet [Takahashi *et al.*, 1993], and temperature of equilibration, Knippa xenoliths come from the uppermost mantle, from depths of 40–70 km. These temperatures are high for a steady state geotherm, except for a lithosphere enriched in heat-producing elements (HPE) near the base of the lithosphere [Stein *et al.*, 1993]. Alternatively, the temperatures may represent transient conditions associated with BIP magmatism. Young and Lee [2009] note that Knippa peridotites are enriched in fluid-mobile trace elements (e.g., La) relative to fluid-immobile trace elements (e.g., Nb). They inferred that such fractionation reflects subduction-related

¹Graduate School of Science and Technology, Shizuoka University, Shizuoka, Japan.

²Institute of Geosciences, Shizuoka University, Shizuoka, Japan.

³Department of Geosciences, University of Texas at Dallas, Richardson, Texas, USA.

⁴Department of Geological Sciences, University of Texas at El Paso, El Paso, Texas, USA.

⁵Department of Geology, Baylor University, Waco, Texas, USA.

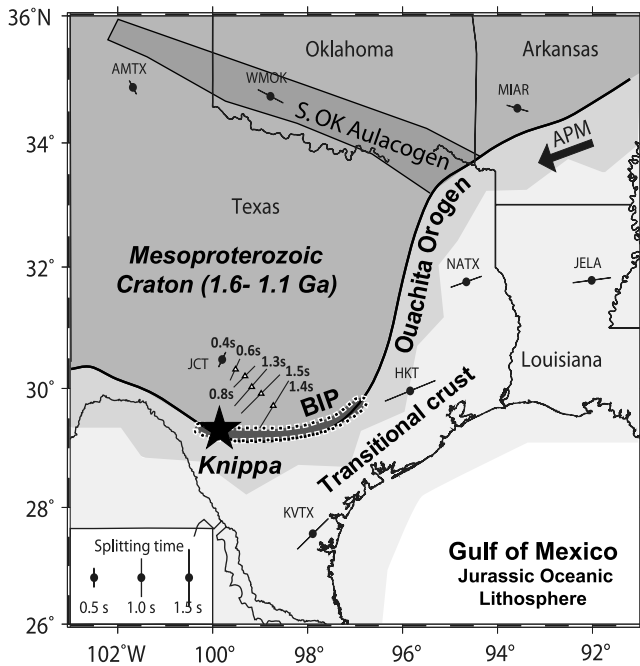


Figure 1. Location of Knippa and principal tectonic features of the south central USA. The peridotite xenoliths are from Knippa quarry in Uvalde County, TX (star). SKS results shows shear-wave splitting time and shear-wave fast directions. Circles, results after Gao *et al.* [2008]; triangles, results from this study (Table 2). The arrow represents the absolute plate motion (APM).

metasomatism of Laurentian lithospheric mantle due to ~1 Ga plate convergence.

3. Microstructural and Fabric Analyses

[6] In this study, we selected eight peridotite xenoliths for detailed petrophysical analyses to evaluate the effect of olivine CPO on seismic-wave properties. The xenoliths are coarse-grained and equigranular, with grain boundaries that range from triple junctions to smoothly curving boundaries. The spinels are elongate, bleb-shaped and dark brown in plane-polarized light. Some spinels and Cpx show corroded rims. Olivine grains are large and commonly contain subgrain boundaries (Figure 2a). Serpentine veins occur in two peridotite xenoliths and cut olivine grains (Figure 2a). These serpentine veins are identified as lizardite by Raman spectroscopy at the University of Tokyo, Japan.

[7] To examine deformation conditions in more detail, we measured the CPOs of olivine grains from highly polished thin sections using a scanning electron microscope equipped with an electron backscatter diffraction system (EBSD), housed at the Center for Instrumental Analysis, Shizuoka University, Japan. We determined Ol, Opx and Cpx crystal orientations, and visually checked the computerized indexation of the diffraction pattern for each crystal orientation.

[8] The dominant slip system in olivine was determined from the orientations of the axes of subgrain rotation and CPO data [e.g., Nicolas and Poirier, 1976; Satsukawa and

Michibayashi, 2009; Katayama *et al.*, 2010]. We rotated the CPO data based on the orientations of the axes of subgrain rotation, such that the “foliation” became horizontal and the “lineation” became E-W (see Text S1 of the auxiliary material for details).¹ Subsequently, using data from the eight xenoliths, we calculated the average sample (1740, 533 and 282 measurements for Ol, Opx and Cpx, respectively), giving the same weight to each measurement, independently of the number of measurements in each xenoliths (Figure 2b and Table 1). As a result, olivine CPO data show a-axis fiber patterns characterized by a strong

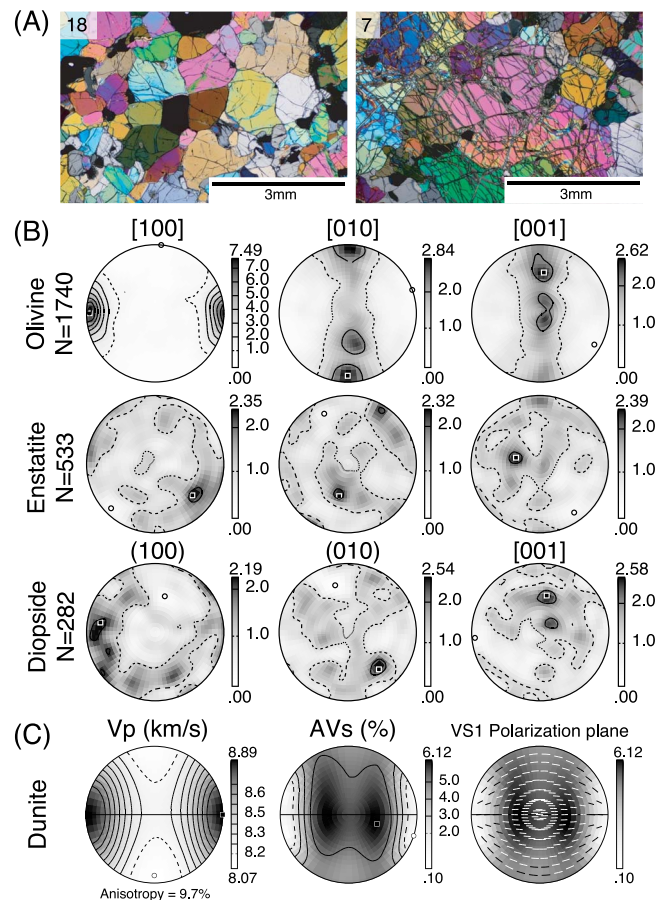


Figure 2. (a) Photomicrographs of Knippa peridotite xenoliths. In some samples, olivines are cut by serpentine veins. Scale bar is 3 mm, 18 and 7 are sample number. (b) CPOs data of the average sample (Table 1) obtained by the EBSD technique. CPOs are plotted on equal-area, lower hemisphere projections. Contours are multiples of the uniform distribution. N is the number of measurements. (c) Seismic properties of the average sample computed from single crystal elastic constants, crystal density, and the average CPOs of olivine. Contours are multiples of uniform density. Vp is 3D distribution of the P-wave velocity. Anisotropy is $(V_{pmax} - V_{pmin}) / V_{pmean}$. AVs (seismic anisotropy of S-waves) is 3D distribution of the polarization anisotropy of S-waves owing to S-wave splitting. Vs1 plane is polarization plane of the fast split S-wave (S1) as a function of the orientation of the incoming wave relative to the structural frame of the sample. Each small segment represents the trace of the polarization plane on the point at which S1 penetrates the hemisphere.

¹Auxiliary materials are available in the HTML. doi:10.1029/2010GL044538.

Table 1. Modal Composition (%), Number of Measurements, J Index Values Calculated After *Mainprice et al.* [2000], and Seismic Properties V_p , AV_p , AV_s , V_{s1} , V_{s2} for the Eight Knippa Peridotite Xenoliths Studied Here^a

Sample Number	Modal Composition				CPO Olivine		Seismic Anisotropy							
	Ol	Opx	Cpx	Sp	N	J	V_p (km/s)		AV_p (%)	AV_s (%)	V_{s1} (km/s)		V_{s2} (km/s)	
							Max	Min		Max	Max	Min	Max	Min
1	63	25	10	2	225	4.60	8.81	8.09	8.4	5.09	4.97	4.86	4.86	4.66
3	69	20	8	3	202	5.29	8.83	8.09	8.7	5.59	5.01	4.84	4.85	4.64
6	70	20	8	2	217	5.55	8.98	8.06	10.8	7.35	5.03	4.84	4.87	4.60
9	82	15	2	1	220	4.61	8.82	8.07	8.9	6.13	4.98	4.84	4.88	4.64
10	80	13	5	2	208	11.42	9.04	8.07	11.3	8.26	5.06	4.82	4.87	4.59
13	68	20	9	3	219	6.05	8.98	8.02	11.4	7.34	5.03	4.86	4.89	4.59
16	81	14	5	1	231	6.67	8.94	8.02	10.8	6.81	5.00	4.85	4.90	4.60
18	75	20	4	1	218	5.94	8.79	7.97	9.8	6.36	5.03	4.80	4.85	4.66
AS (D)	100	0	0	0	1740	-	8.89	8.07	9.7	6.12	5.01	4.84	4.87	4.63
AS (H)	80	15	5	0	-	-	8.75	8.08	7.9	4.92	4.97	4.84	4.86	4.67
AS (L)	70	18	12	0	-	-	8.89	8.07	7.1	4.35	4.95	4.83	4.85	4.68

^aN, number of measurements; J , J index; MD, maximum density; AS, average sample; D, dunite; H, harzburgite; L, lherzolite. The last three lines report the average sample. The average sample has been calculated from the sum of all measurements, giving the same weight to each measurement.

concentration in [100] with weak girdles of [010] and [001], whereas the CPOs of enstatite and diopside show nearly random fabrics (Figure 2b).

4. Rock Seismic Properties

[9] We calculated the seismic properties of the peridotite xenoliths from single crystal elastic constants, crystal density, and the CPO of Ol, Opx, and Cpx, assuming different scenarios: either a composition of 100% Ol (for each sample as well as the mean), or the actual modal composition of the rock (dunite, lherzolite and harzburgite). The elastic constants and averaging scheme used in our calculations are same in the work of *Michibayashi et al.* [2009].

[10] Figure 2c and Table 1 presents the seismic properties of the peridotite xenoliths. The maximum seismic anisotropy of S-waves varies between 5.09 and 8.26% for 100% olivine, whereas average samples vary between 4.35 and 6.12% along with variations of mineral composition (Table 1). Polarization anisotropies of most samples have two maxima girdles on each side of a plane normal to the [100] maximum, whereas the minimum birefringence occurs for propagation directions close to the [100] maximum (Figure 2c). The orientation of the polarization plane of the fastest S-wave systematically marks the orientation of the great circle that contains the maximum concentration of [100] (Figure 2b). These anisotropic patterns are quite common globally, as previously reported [e.g., *Mainprice et al.*, 2000].

5. Seismic Data

[11] Five broadband, three-component seismographs were deployed between Junction and San Antonio, TX from February through August 2008 at an average spacing of 28 km (Table 2) [*Pulliam et al.*, 2009]. The transect extended from the Laurentian craton to the edge of the craton and, possibly, onto the stretched and thinned transitional crust of the Texas Gulf Coastal Plain. Receiver function results for the same stations indicate crustal thickness of 32 km at GCP05 vs. 45 km at GC01 [*Pulliam et al.*, 2009].

[12] For each temporary station, as well as for the permanent ANSS station JCT, SKS splitting measurements were made for 22 deep-focus ($h > 50$ km) teleseismic events with magnitudes greater than 6.0 using the Matlab-based

SplitLab software [*Wüstefeld et al.*, 2008]. SplitLab simultaneously computes splitting parameters via three independent techniques: (a) the rotation-correlation method [e.g., *Bowman and Ando*, 1987], which maximizes the cross-correlation between the radial and transverse component of the SKS phase, (b) the minimum energy method [*Silver and Chan*, 1991], which minimizes the energy on the transverse component, and (c) the minimum eigenvalue method [*Silver and Chan*, 1991].

[13] For measurements to be accepted we required that results for both the minimum energy and rotation-correlation methods each display clear minima in their error surfaces and be consistent with each other, i.e., within 0.2 s of delay time and 20° with respect to fast polarization direction. On average, only five events satisfied these criteria for our stations during their seven-month deployment. Figure 1 shows averaged results for the best five events at each station, including the permanent station JCT, located near Junction, TX. Our results for Junction (Table 2) confirm the results reported previously by *Gao et al.* [2008]. Results from the five temporary stations show rapidly increasing delay times but only small changes in the fast polarization direction as one progresses from Junction toward the southeast.

6. Discussion and Conclusions

[14] The region that spans the northern GoM margin underwent two complete cycles of continental rifting (ca. 540 and 170 Ma) and collisional orogeny (ca. 1000 and

Table 2. Station Locations and SKS Splitting Results From the 2008 Broadband Deployment^a

Station	Latitude (deg)	Longitude (deg)	Elevation (m)	Sensor	δt	Φ
JCT	30.48	-99.8	581	Streckeisen STS2	0.42	28
GC01	30.33	-99.53	681	Guralp CMG-3ESP	0.57	24
GC02	30.2	-99.34	634	Guralp CMG-3ESP	0.8	44
GC03	30.02	-99.21	598	Guralp CMG-3T	1.3	42
GC04	29.91	-99.01	487	Guralp CMG-3ESP	1.5	46
GC05	29.73	-98.74	468	Guralp CMG-3ESP	1.44	34

^aDelay times between the fast and slow polarization directions are indicated by δt ; the orientation of the fast polarization direction, with respect to north, is indicated by Φ .

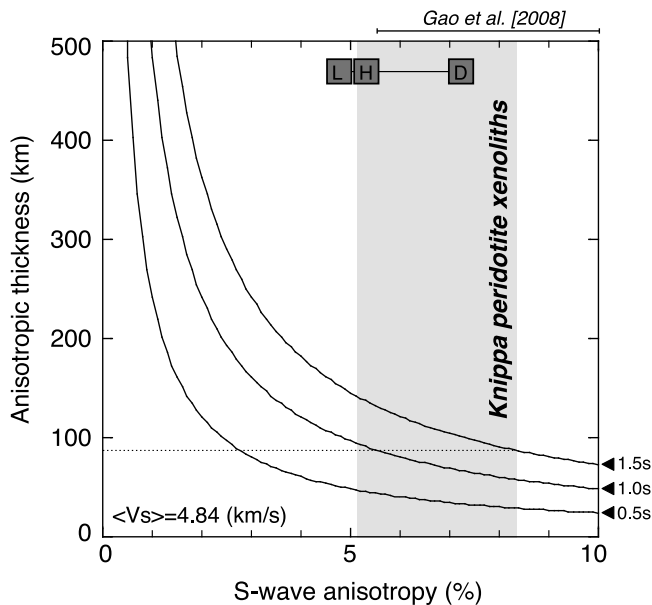


Figure 3. Relationship between S-wave anisotropy (AVs) and required thickness of anisotropic layer in Knippa peridotite xenoliths calculated as 100% olivine. Shear-wave splitting time is 0.5 to 1.5 s, from Gao *et al.* [2008]. Gray area shows the range of AVs obtained by individual samples. D, H and L are dunite harzburgite, lherzolite of average sample shown in Table 1.

350 Ma) along the southern flank of Laurentia [e.g., Thomas, 2006]. These events include the late Mesoproterozoic Grenville orogeny, early Cambrian rifting and passive margin formation, late Paleozoic Ouachita orogeny during the final stages of assembly of Pangaea, and formation of the modern continental margin accompanied by brief sea-floor spreading and oceanic crust formation during the Jurassic (ca. 165 Ma).

[15] The lithosphere that formed or was reworked during these tectonics events is preserved across a region that extends from the Grenville province of the craton [Anthony, 2005] to Jurassic oceanic crust in the GoM. The Moho beneath the Texas passive margin is approximately 40 km deep [Gao *et al.*, 2008]. As described above, Knippa peridotites come from 40–70 km deep [Raye *et al.*, 2009]. Therefore, we consider it likely that the Knippa peridotite xenoliths are derived from the uppermost mantle lithosphere. We note that the region is dominated by alternate episodes of extension and compression (Figure 1). The associated mantle fabric could preserve some of this deformation, suggesting an important potential for tectonic inheritance and overprinting.

[16] The strong gradient in shear wave splitting observed along the traverse near Knippa implies a shallow, i.e. lithospheric, source for the anisotropy. One possible explanation invokes flow in the lithospheric mantle as a mechanism for aligning olivine fast axes: the Coastal Plain appears to have a crust that is on the order of 10 km thinner than the craton [Mickus *et al.*, 2009]. This would allow a correspondingly thicker lithospheric mantle and, therefore, longer paths for SKS to accumulate splitting times, assuming flow channeled around the cratonic keel aligns crystals' a-axes effectively.

[17] Gao *et al.* [2008] argued that the magnitude of anisotropy must be 5.5–10% (Figure 3) in order to produce the observed 0.9 to 1.6 s splitting time, assuming that the lithosphere beneath the region is 70 km thick (Figure 1). Our measurements constrain the intrinsic anisotropy within the lithospheric mantle, although the original orientations of the peridotite xenoliths were lost during their volcanic transport to the surface [e.g., Michibayashi *et al.*, 2009]. As noted above, the average Knippa peridotite shows 4.35 to 6.12% anisotropy depending on mineral compositions, whereas individual samples vary range from 5.09 to 8.26% in case of Ol 100% (Figure 3). Consequently, the observed delay times are mostly explained by the seismic properties of the mantle lithosphere sampled by Knippa peridotite xenoliths.

[18] To explain the variation of splitting time near station JCT is complicated. The thickness (T) of an anisotropic layer is given by $T = (100 \text{ dt} \langle V_s \rangle) / AV_s$, [e.g., Pera *et al.*, 2003]. Accordingly, the observed delay time (0.5–1.5 s at JCT) can be explained by the seismic properties of our peridotite xenoliths for an approximately 50 to 150 km thickness. However, it is difficult to produce the observed variation in split times over lateral distances of a few tens of km with this explanation alone. For example, if we use the AVs of a highly deformed sample (sample number; 10 shown in Table 1), the long delay time (1.5 s) requires 85 km thickness. Therefore, a more likely candidate is deformation caused by collision between Laurentia and Gondwana during the late Paleozoic, which produced large amounts of deformation, including the folded Ouachita mountain chain. Varying amounts of deformation would produce corresponding variations in the alignment of olivine fast directions in the lithospheric mantle. Such deformation can both vary significantly over short distances and can vary in its effectiveness in aligning crystals. In the case of Oman ophiolites, major shear zones seem to have developed at the contact between a flowing asthenosphere (young) and a frozen lithospheric (old) wall, a thermal boundary inducing a characteristic asymmetry [Nicolas and Boudier, 2008]. Consequently, the long delay time can be explained by fabric variation, that is, peridotites beneath the transitional crust could preserve greater deformation from the Paleozoic Ouachita orogeny (young) rather than the lithosphere beneath the Mesoproterozoic craton (old). Overall, the Knippa peridotite xenoliths demonstrate the possible occurrence of an anisotropic layer in the uppermost mantle lithosphere that could be related to ‘frozen’ deformation associated with the alternate processes of extension and compression beneath the southern Laurentian margin.

[19] **Acknowledgments.** Drawings of CPO and calculations of *J* index and seismic anisotropy were performed using the interactive programs of D. Mainprice of Université Montpellier II, France. We are grateful to H. Kagi of University of Tokyo, Japan, for his assistance during Raman spectra analyses. This work was supported by a grant-in-aid for scientific research (223708) by the JSPS Research Fellowships for Young Scientists (to T.S.), research grant (19340148, 22244062) by the JSPS (to K.M.), the Texas Advanced Research Program (to E.Y.A. and R.J.S.), and EAR-0750711 by the U.S. NSF (to J.P., E.Y.A., and R.J.S.).

References

Anthony, E. Y. (2005), Source regions of granites and their links to tectonic environment: Examples from the western United States, *Lithos*, 80, 61–74, doi:10.1016/j.lithos.2004.04.058.

- Bowman, J. R., and M. Ando (1987), Shear-wave splitting in the upper-mantle wedge above the Tonga subduction zone, *Geophys. J. R. Astron. Soc.*, *88*, 25–41.
- Brey, G. P., and T. Kohler (1990), Geothermobarometry in four-phase lherzolites II. New thermobarometers, and practical assessment of existing thermobarometers, *J. Petrol.*, *31*, 1353–1378.
- Fouch, M. J., and S. Rondenay (2006), Seismic anisotropy beneath stable continental interiors, *Phys. Earth Planet. Inter.*, *158*, 292–320, doi:10.1016/j.pepi.2006.03.024.
- Gao, S. S., K. H. Liu, R. J. Stern, G. R. Keller, J. P. Hogan, J. Pullian, and E. Y. Anthony (2008), Characteristics of mantle fabrics beneath the south-central United states: Constraints from shear-wave splitting measurements, *Geosphere*, *4*(2), 411–417, doi:10.1130/GES00159.1.
- Griffin, W. R., K. A. Foland, R. J. Stern, and M. L. Leybourne (2010), Geochronology of bimodal alkaline volcanism in the Balcones Igneous Province, Texas: Implications for Cretaceous intraplate magmatism in the northern Gulf of Mexico magmatic zone, *J. Geol.*, *118*, 1–21, doi:10.1086/648532.
- Katayama, I., K. Michibayashi, R. Terao, J. Ando, and T. Komiya (2010), Water content of the mantle xenoliths from Kimberley and implications for explaining textural variations in cratonic roots, *Geol. J.*, doi:10.1002/gj.1216, in press.
- Keller, G. R., J. M. Kruger, K. J. Smith, and W. M. Voight (1989), The Ouachita system: A geophysical overview, in *The Appalachian–Ouachita Orogen in the United States*, *Geol. North Am.*, vol. F2, edited by R. D. Hatcher Jr. et al., pp. 689–694, Geol. Soc. Am., Boulder, Colo.
- Mainprice, D., G. Barruol, and W. Ben Ismaïl (2000), The anisotropy of the Earth's mantle: From single crystal to polycrystal, in *Mineral Physics and Seismic Tomography: From Atomic to Global*, *Geophys. Monogr. Ser.*, vol. 117, edited by S. Karato et al., pp. 237–264, AGU, Washington, D. C.
- Michibayashi, K., T. Oohara, T. Satsukawa, S. Ishimaru, A. Arai, and V. M. Okrugin (2009), Rock seismic anisotropy of the low velocity zone beneath the volcanic front in the mantle wedge, *Geophys. Res. Lett.*, *36*, L12305, doi:10.1029/2009GL038527.
- Mickus, K., R. J. Stern, G. R. Keller, and E. Y. Anthony (2009), Potential field evidence for a volcanic rifted margin along the Texas Gulf Coast, *Geology*, *37*, 387–390, doi:10.1130/G25465A.1.
- Nicolas, A., and F. Boudier (2008), Large shear zones with no relative displacement, *Terra Nova*, *20*(3), 200–205, doi:10.1111/j.1365-3121.2008.00806.x.
- Nicolas, A., and N. I. Christensen (1987), Formation of anisotropy in upper mantle peridotites: A review, in *Composition, Structure and Dynamics of the Lithosphere-Asthenosphere System*, *Geodyn. Ser.*, vol. 16, edited by K. Fuchs and C. Froidevaux, pp. 111–123, AGU, Washington, D. C.
- Nicolas, A., and J. P. Poirier (1976), *Crystalline Plasticity and Solid State Flow in Metamorphic Rocks*, 444 pp., John Wiley, New York.
- Pera, E., D. Mainprice, and L. Burlini (2003), Anisotropic seismic properties of the upper mantle beneath the Torre Alfina area (northern Apennines, central Italy), *Tectonophysics*, *370*, 11–30, doi:10.1016/S0040-1951(03)00175-6.
- Pulliam, J., S. Suhardja, R. J. Stern, E. Anthony, S. Gao, G. R. Keller, and K. Mickus (2009), Broadband seismic study of the Texas continent-ocean boundary: A pilot project, paper presented at 43rd Annual Meeting, Geol. Soc. of Am., Richardson, Tex., 16–17 March.
- Raye, U., R. J. Stern, E. Y. Anthony, M. Ren, J. Kimura, K. Tani, and C. Qing (2009), Characterization of mantle beneath Texas: Constraints from Knippa xenoliths, *Geol. Soc. Am. Abstr. Programs*, *41*(2), 29.
- Satsukawa, T., and K. Michibayashi (2009), Determination of slip system in olivine based on crystallographic preferred orientation and subgrain-rotation axis: Examples from Ichinomegata peridotite xenoliths, Oga peninsula, Akita prefecture, *J. Geol. Soc. Jpn.*, *115*, 288–291.
- Silver, P. G., and W. W. Chan (1991), Shear wave splitting and subcontinental mantle deformation, *J. Geophys. Res.*, *96*, 16,429–16,454, doi:10.1029/91JB00899.
- Stein, M., Z. Garfunkel, and E. Jagoutz (1993), Chronothermometry of peridotitic and pyroxenitic xenoliths: Implications for the thermal evolution of the Arabian lithosphere, *Geochim. Cosmochim. Acta*, *57*, 1325–1337, doi:10.1016/0016-7037(93)90069-9.
- Takahashi, E., T. Shimazaki, Y. Tsuzaki, and H. Yoshida (1993), Melting study of a peridotite KLB-1 to 6.5 GPa, and the origin of basaltic magmas, *Philos. Trans. R. Soc. London, A*, *342*, 105–120, doi:10.1098/rsta.1993.0008.
- Thomas, W. A. (2006), Tectonic inheritance at a continental margin, *GSA Today*, *16*, 4–11, doi:10.1130/1052-5173(2006)016[4:TIAACM]2.0.CO;2.
- Wüstefeld, A., G. Bokelmann, C. Zarol, and G. Barruol (2008), SplitLab: A shear-wave splitting environment in Matlab, *Comput. Geosci.*, *34*(5), 515–528, doi:10.1016/j.cageo.2007.08.002.
- Young, H. P., and C.-T. A. Lee (2009), Fluid-metasomatized mantle beneath the Ouachita belt of southern Laurentia: Fate of lithospheric mantle in a continental orogenic belt, *Lithosphere*, *1*, 370–383, doi:10.1130/L72.1.

E. Y. Anthony, Department of Geological Sciences, University of Texas at El Paso, El Paso, TX 79968, USA.

K. Michibayashi and T. Satsukawa, Graduate School of Science and Technology, Shizuoka University, Shizuoka 422-8529, Japan. (f5944004@ipc.shizuoka.ac.jp)

J. Pulliam, Department of Geology, Baylor University, Waco, TX 76798, USA.

U. Raye and R. Stern, Department of Geosciences, University of Texas at Dallas, Richardson, TX 75080, USA.